Technical Report: Optimal Current Trajectories for Power Converters with Minimal Common Mode Voltage

Peter Hokayem * Ivan Pejcic † Nikolaos Oikonomou *

April 2, 2017

Abstract

This article addresses the topic of computing optimized pulse patterns with common mode voltage constraints. The main thrust is to obtain tractable reformulations of the CMV constraints in the frequency domain in order to avoid complex mixed time-frequency formulations. The resulting optimization problem is a nonlinear one for which efficient numerical solvers are readily available. Moreover, we provide an algorithmic way of reducing the conservatism in the reformulated problem and validate our method with numerical illustrations that highlight the benefit of the proposed approach.

1 Introduction

Optimized pulse patterns (OPPs) or optimized Pulse Width Modulation (PWM) based schemes have a long history in the field of control of power converters, see, for example Buja (1980); Holtz and Qi (2013) and references therein. OPPs are extensively used since they tend to provide optimal current Total Demand Distortion (TDD) at the output of multilevel inverters for a fixed switching frequency. This latter property, i.e., fixed switching frequency, makes the usage of OPPs in the control of power converters even more attractive, as it limits the switching losses and hence improves the overall efficiency.

*ABB Corporate Research Center, Segelhofstrasse 1K, Baden-Dättwil, 5405 Switzerland, {peter.al-hokayem,nikolaos.oikonomou}@ch.abb.com.

†Laboratoire d'Automatique, École Polytechnique Fédérale de Lausanne, 1015 Lausanne, Switzerland, ivan.pejcic@epfl.ch.

Pulse width modulation techniques for controlling power converters have been extensively studied, see Holmes and Lipo (2003) for an authoritative reference on the analysis of PWM methods. Optimal PWM methods or equivalently OPP methods are a subclass of PWM methods in which the switch signals are computed offline, based on a certain performance criterion - typically minimal current TDD - and a set of constraints on the fundamental component as well as the individual harmonics. In particular, Selective Harmonic Elimination (SHE) is one technique in which the switching angles are designed so that the maximal possible number of harmonics is eliminated, and hence the current TDD may be improved in this way Fei et al. (2009); Agelidis et al. (2008); Chiasson et al. (2008). There have been also many proposals on computing OPPs without SHE, for example in Meili et al. (2006). Control methods of power converters using OPPs as the main ingredient have appeared in Geyer et al. (2010, 2012); Holtz and Oikonomou (2007); Holtz and Beyer (1995, 1991); Rathore et al. (2013).

Computing OPPs *with* limited Common Mode Voltage (CMV) is a topic that has been rarely addressed, although it is of high importance. OPPs with reduced CMV lead to a better lifetime of the electric machine as they reduce the stress on the machine insulation. This extra benefit comes at the expense of an extra constraint to be incorporated into the optimization problem that generates the OPPs; this constraint is of a nonlinear nature and is a time-domain expression. In this article, we focus on generating OPPs for L-level converters with the CMV constraint and obtain tractable reformulations of the CMV constraint. These reformulations of the CMV constraint allow us to use either the Fourier coefficients that represent the OPPs for any L-level converter or the switching angles in the special case of 3-level converters.

This paper is organized as follows. Section 2 presents the problem of designing OPPs with minimal current TDD and a constraint on the CMV. We present various convex reformulations of the CMV constraint in the frequency domain in Section 3. We then present numerical results in Section 4, illustrating the conservatism of the various constraint reformulations. Finally, we conclude in Section 5 and provide directions for future work.

2 Problem Formulation

Consider an L-level converter (Figure 1) operated using OPPs. Referring to Figure 2, denote by $v(t) = v(\omega_1 t)$ an OPP waveform, where $\omega_1 = 2\pi f_1 = \frac{2\pi}{T_1}$ and f_1 is the fundamental frequency. Without any loss of generality, we shall take $\omega_1 = 1$; however, the results in the paper remain valid for any choice of ω_1. The signal $v(t)$ is described by a sequence of switching angles $\bar{\alpha} = \left[\alpha_1, \alpha_2, \cdots, \alpha_N\right]$ and the

corresponding jumps in the voltage levels $\bar{f} = \left[f_1, f_2, \cdots, f_N\right]$, where

$$f_i = \begin{cases} +1, & \text{for a rising edge,} \\ -1, & \text{for a falling edge,} \end{cases} \tag{1}$$

and N is the so-called pulse number. We shall restrict our attention to OPPs with the following three properties.

P1. *Quarter wave symmetry*: the following two conditions hold $v(t) = v(\pi - t), \quad \forall t \in \left[0, \frac{\pi}{2}\right]$ and $v(t) = -v(2\pi - t), \quad \forall t \in \left[0, \pi\right]$.

P2. *Three phase symmetry*:

$$\begin{aligned} v_a(t) &= v(t), \\ v_b(t) &= v\left(t - \tfrac{2\pi}{3}\right), \\ v_c(t) &= v\left(t + \tfrac{2\pi}{3}\right). \end{aligned} \tag{2}$$

P3. $v_a(t) \geq 0, \forall t \in [0, \pi/2]$.

Given the quarter wave symmetry, property (P1) and the fact that only single level jumps are allowed in the OPP, i.e., (1) holds, the Fourier series expansion of a single phase OPP is given by

$$v(t) = \sum_{k=1,3,5,\cdots} \hat{v}_k \sin(kt), \tag{3}$$

where $\hat{v}_k$ is the amplitude (Fourier coefficient) of k-th voltage harmonic given by

$$\hat{v}_k = \frac{4}{\pi} \frac{u_d}{(L-1)} \frac{1}{k} \sum_{i=1}^{N} f_i \cos(k\alpha_i), \tag{4}$$

where u_d is the full DC link voltage in an L-level converter. The derivation of (4) may be found in the Appendix.

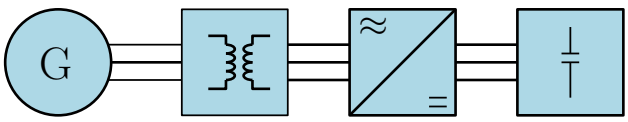

Figure 1: A setup in which an inverter unit converts DC to AC signals to drive an electric machine.

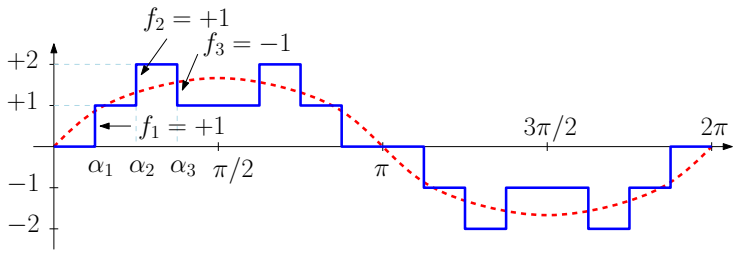

Figure 2: An example of a pulse pattern $v(t)$ with $N = 3$ for a 5-level converter.

2.1 Performance Index

Assuming that the OPPs are used to drive a machine with a Y-connection, then the 3 phase currents are driven by the voltages $v_{a0} = v_a - v_0$, $v_{b0} = v_b - v_0$ and $v_{c0} = v_c - v_0$, where

$$v_0(t) = \frac{1}{3}\left(v_a(t) + v_b(t) + v_c(t)\right) \tag{5}$$

is the common mode voltage (CMV) at the star point connection of the machine. Since v_0 contains all triple harmonics, these harmonics are absent from the current signals. Accordingly, we can define the current TDD as

$$TDD_i = \frac{1}{I_{rat}} \sqrt{\sum_{k \in \mathbb{H}_{TDD}} \left(\hat{i}_k\right)^2}, \tag{6}$$

where I_{rat} is the rated peak value of current, and $\mathbb{H}_{TDD} := \{5, 7, 11, 13, \cdots\}$. Assuming that the response of the induction machine at harmonics $\hat{v}_k$ beyond the fundamental can be modeled as a pure leakage inductance l_σ, i.e., the resistance is negligible, the current harmonics can be approximated by $\hat{i}_k \approx \frac{\hat{v}_k}{k l_\sigma}$. Upon substituting this expression into (6), we obtain the following expression

$TDD_i \approx \frac{1}{l_\sigma I_{rat}} \sqrt{\sum_{k \in \mathbb{H}_{tdd}} \left(\frac{\hat{v}_k}{k}\right)^2}$

$= \frac{1}{l_\sigma I_{rat}} \frac{4u_d}{\pi(L-1)} \sqrt{\sum_{k \in \mathbb{H}_{tdd}} \left[\frac{1}{k^4}\left(\sum_{i=1}^{N} f_i \cos(k\alpha_i)\right)^2\right]}$. The nonlinear performance index TDD_i is to be minimized to obtain the optimal sequence $\bar{f}^* := \left[f_1^*, f_2^*, \cdots, f_N^*\right]$ and the corresponding set of optimal switching angles $\bar{\alpha}^* := \left[\alpha_1^*, \alpha_2^*, \cdots, \alpha_N^*\right]$, under a specific set of constraints that are discussed next.

2.2 Constraints

Foremost, one is interested in keeping the fundamental component of the Fourier series at a specific level (the modulation index m), i.e.,

$$\hat{v}_1 = m. \tag{7}$$

Another constraint may be related to the amplitude of individual harmonics in relation to the fundamental. This can be posed as

$$|\hat{v}_k| \leq \rho_k |\hat{v}_1| \tag{8}$$

where ρ_k's are some nonnegative factors. The constraint (8) is very useful when dealing with rectifier units as it allows the satisfaction of grid codes in terms of harmonic emissions into the grid.

One may also be interested in enforcing a constraint pertaining to the minimal separation between any two consecutive switches over a single phase, i.e.,

$$\begin{cases} 0 \leq \alpha_1 \leq \cdots \leq \alpha_N \leq \frac{\pi}{2}, \\ \alpha_{i-1} + \delta \leq \alpha_i, \quad \forall i \in \{2, \ldots, N\}, \end{cases} \tag{9}$$

where δ is the minimal separation between any two consecutive switching angles.

Assuming that the three phase symmetry (2) holds, then the CMV (5) can be written as

$$v_0(t) = \sum_{k \in \mathbb{H}_0} \hat{v}_k \sin(kt), \tag{10}$$

where $\mathbb{H}_0 = \{3, 9, 15, 21, 27, \cdots\}$ is the index set of the tripplen harmonics (multiples of 3 that are not even) that are present in the CMV; we show this fact in the Appendix. The constraint on the CMV can now be defined as

$$|v_0(t)| = \left| \sum_{k \in \mathbb{H}_0} \hat{v}_k \sin(kt) \right| \leq \gamma, \tag{11}$$

where γ represents the maximally allowed bound on the CMV. Interesting to note, that due to the switched nature of the OPPs, the resulting CMV can only be equal to 0 or an integer multiple of $\frac{1}{3}$.

It is important to note here that none of the constraints (9), (7), and (8) pose changes to the forthcoming discussion in the paper, as the discussion pertains mainly to the approximation of the CMV constraint (11).

2.3 Optimization Problem

The resulting optimization problem for generating OPPs with minimal current TDD and limited CMV is given by

$$\min_{(f_1,\cdots,f_N,\alpha_1,\cdots,\alpha_N)} \quad TDD_i$$
$$\text{subject to} \begin{cases} \hat{v}_1 = m, \\ |\hat{v}_k| \leq \rho_k |\hat{v}_1|, \\ 0 \leq \alpha_1 \leq \cdots \leq \alpha_N \leq \frac{\pi}{2}, \\ \alpha_{i-1} + \delta \leq \alpha_i, \quad \forall i \in \{2,\ldots,N\}, \\ |v_0(t)| \leq \gamma. \end{cases} \tag{12}$$

The optimization problem (12) involves integer decision variables $(f_1,\cdots,f_N)$ representing the structure of the OPP waveform, and as such it is of a mixed integer nonlinear program (MINLP) type. For a selected number of pulses N of an L-level inverter, there exists a finite set of allowed structures which can be enumerated. Hence, for each fixed choice of the structure we can solve (12) to obtain the optimal set of angles. Subsequently, we can post-process the data to obtain the best solution over the various structures. This way we would have to solve a finite number of nonlinear programs (NLP) for which efficient solvers are available.

3 Convex Reformulations of the Zero Sequence Constraint

The constraint (11) involves the time t, and as such problem (12) comprises a mixture of amplitudes of harmonics, as well as time domain signals, which makes it very difficult to directly tackle the problem.

One approach is to combine equations (3), (5) and (11), and grid the resulting constraint over the time t. However, this would produce a huge number of constraints that *approximate* that original one (11); moreover, the satisfaction of the large amount of extra constraints does not necessarily mean the satisfcation of the original one (11). As such, we opt for a method that translates the time-domain constraint (11) into a slightly more conservative constraint on the magnitude of the harmonics.

3.1 ℓ_1/ℓ_2-Norm Approximations

Consider again the constraint (11). In order to avoid the griding approach over the time variable t, we apply the following steps to upper-bound the original constraint

$$\begin{aligned}\left|\sum_{k\in\mathbb{H}_0}\hat{v}_k\sin(kt)\right| &\leq \sum_{k\in\mathbb{H}_0}|\hat{v}_k\sin(kt)| \leq \sum_{k\in\mathbb{H}_0}|\hat{v}_k|\,|\sin(kt)| \\ &\leq \sum_{k\in\mathbb{H}_0}|\hat{v}_k| = \left\|\begin{bmatrix}\hat{v}_3 & \hat{v}_9 & \dots & \hat{v}_{99}\end{bmatrix}\right\|_1 \leq \gamma. \end{aligned} \tag{13}$$

Now the satisfaction of the inequality (13), in terms of the ℓ_1-norm *implies* the satisfaction of the original constraint (11). Of course, this would imply taking an infinite number of harmonics that are in $\mathbb{H}_0$. However, since the amplitudes $\hat{v}_k$ are according to equation (4) inversely proportional to the harmonic order k, the infinite sum can be reasonably well approximated by truncating the set $\mathbb{H}_0$. For example, we could take the following set of harmonics $\tilde{\mathbb{H}}_0 = \{3,9,15,\cdots,99\}$, and hence rewrite the constraint (13) as

$$\left\|\begin{bmatrix}\hat{v}_3 & \hat{v}_9 & \dots & \hat{v}_{99}\end{bmatrix}\right\|_1 = \sum_{k\in\tilde{\mathbb{H}}_0}|\hat{v}_k| \leq \gamma. \tag{14}$$

Another alternative would be to have an ℓ_2-norm formulation, which is computed based on the following relationship between the two types of norms Khalil (2001)

$$\|v\|_2 \leq \|v\|_1 \leq \sqrt{n}\,\|v\|_2\,, \tag{15}$$

where n is the dimension of the vector v. Applying the second inequality in (15) to the constraint (14), results in

$$\left\|\begin{bmatrix}\hat{v}_3 & \hat{v}_9 & \dots & \hat{v}_{99}\end{bmatrix}\right\|_2 = \sqrt{\sum_{k\in\tilde{\mathbb{H}}_0}|\hat{v}_k|^2} \leq \frac{\gamma}{\sqrt{\#(\tilde{\mathbb{H}}_0)}}, \tag{16}$$

where $\#(\tilde{\mathbb{H}}_0)$ indicates the number of elements in the set $\tilde{\mathbb{H}}_0$. Hence the satisfaction of the constraint (16) implies the sanctification of the constraint (14), which in turn implies the satisfaction of the original constraint (11), assuming of course that the cardinality of the set $\tilde{\mathbb{H}}_0$ is high enough.

We conclude this section with a few remarks on the foregoing approximations of the CMV constraint: (14) is a linear constraint in the harmonic amplitudes $\hat{v}_k$, while (16) is a quadratic one. However, both constraints are finally nonlinear in terms of the decision variables, i.e., the angles α_i. The constraints (16) and (14) are an approximation of the original constraint (11). Although (16) is more conservative than (14), it could be in practice that the former can provide a better

answer to the problem due to the shape of the two norms. This is due to the fact that we are dealing with nonlinear problems, and that the certain initial conditions of the switching angles may result in triple harmonics amplitudes that are contained the the ℓ_2-norm version and not in the ℓ_1-norm.

The results in this section lead to the following Algorithm 1.

Algorithm 1 Computing OPPs with CMV Constraints

Require: N, L, γ_{max}, $\#\mathbb{H}_{tdd}$, $\#\mathbb{H}_0$, γ_0, $m_{\min}$, $m_{\max}$, and M;

1: Generate an ordered set of M modulation indices $\{m_1, \cdots m_M\}$ within the range $[m_{\min}, m_{\max}]$;
2: Generate the set of all possible switching patterns $\bar{f}_1, \cdots, \bar{f}_K$, using N and L;
3: **for** i=1 to M **do**
4: **for** k=1 to K **do**
5: Set $\gamma = \gamma_0$;
6: **while** $\gamma \leq \gamma_{\max}$ **do**
7: Solve the following optimization problem:

$$\begin{aligned} \min_{\bar{\alpha}} \quad & TDD_i(\bar{f}_k, \bar{\alpha}) \\ \text{subject to} \quad & (7), (8), (9), \text{ and either (14) or (16);} \end{aligned}$$

8: Check if the optimal solution satisfies (11) with γ_0 as an upper bound and retain the feasible solutions only;
9: Set $\gamma = \gamma + \frac{1}{3}$;
10: **end while**
11: **end for**
12: Check for the solution $(\bar{\alpha}^*(i), \bar{f}^*(i))$ with the best TDD_i;
13: **end for**

3.2 Special Cases for L=3

For the case of a 3-level converter, it can be easily seen that there holds $v_0(t) \in \{-1,\ -2/3,\ -1/3,\ 0,\ 1/3,\ 2/3,\ 1\}$. Furthermore, by considering only patterns which have non-negative values in the first half of the period, the set of possible CMV values reduces to $\{-2/3, -1/3, 0, 1/3, 2/3\}$. As such, we would like to see if there are 'simpler' constraints in this case on the angles that would imply the satisfaction of (11). Before we propose our solution for approximating constraint (11), it is important to note that due to our assumptions P1-P2, the CMV in (5) has a period of $\frac{2\pi}{3}$ (this follows from (10)) and is again quarter-wave symmetric over this period. As such, it is sufficient to look at the evolution of the CMV over

the range $\left[0, \frac{\pi}{6}\right]$. Moreover, we can show that the constraint (11) is equivalent (without any conservatism) to the following constraint

$$|v_0(t)| = \frac{\left|v(t) + v\left(\frac{\pi}{3} - t\right) - v\left(\frac{\pi}{3} + t\right)\right|}{3} \leq \gamma, \tag{17}$$

$\forall t \in \left[0, \frac{\pi}{6}\right]$. The proofs of the foregoing facts are provided in the Appendix. To our knowledge, this is the first time the equivalent constraint of this form has been noted in the literature. However, this equivalent constraint (17) is still very difficult to solve as it involves integer variables indicating in which of the intervals $\left[0, \frac{\pi}{6}\right]$, $\left[\frac{\pi}{6}, \frac{\pi}{3}\right]$ and $\left[\frac{\pi}{3}, \frac{\pi}{2}\right]$ each angle α_i falls. The condition (17) states that the

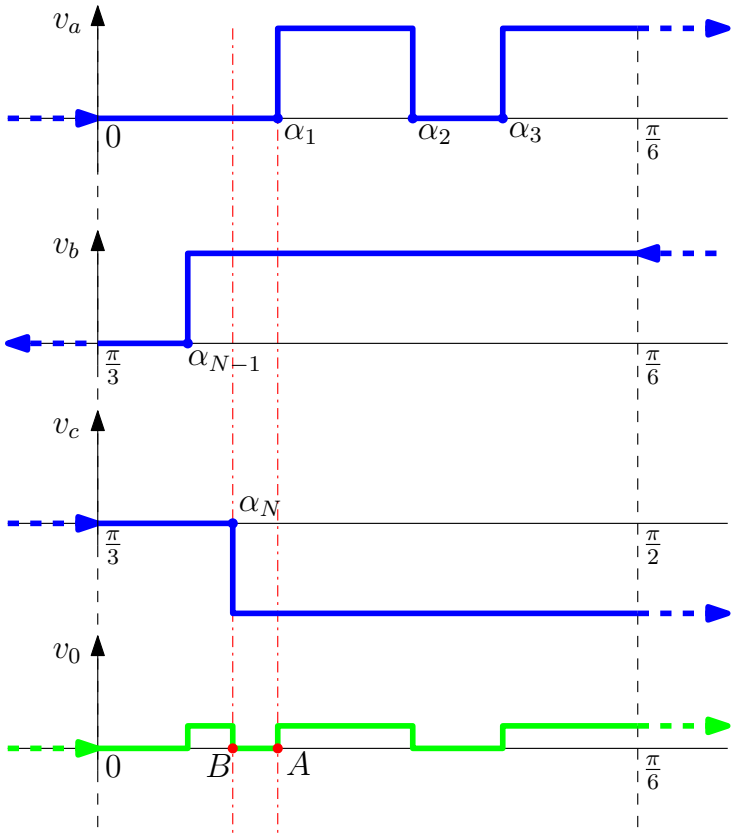

Figure 3: An example illustrating the result in Proposition 3. An instance where the last switching angle α_5 falls between 60 and 90 degrees, and the constraint in Proposition 3 implies that the point A falls after the point B. This figure also illustrates the relationship (17) for a 3-level OPP.

CMV voltage can be characterized by adding the part of the OPP in the interval $\left[0, \frac{\pi}{6}\right]$ to the mirrored version of the OPP in the interval $\left[\frac{\pi}{6}, \frac{\pi}{3}\right]$, and then subtracting from the answer the part of the OPP in the interval $\left[\frac{\pi}{3}, \frac{\pi}{2}\right]$, as depicted in

Figure 3 for a generic 3 Level OPP. The condition (17) leads to the following set of results that give sufficient linear constraints on the angles α_i's which imply a bound of $\gamma = \frac{1}{3}$ on the CMV.

Proposition 1 *For a 3-level OPP, if* $\alpha_1 \geq \frac{\pi}{6}$ *then* $|v_0(t)| \leq \frac{1}{3}$.

Proof. If $\alpha_1 \geq \frac{\pi}{6}$ then $v(t) = 0, \forall t \in \left[0, \frac{\pi}{6}\right]$, and the value of $v(t)$ is either 0 or 1 on the intervals $\left[\frac{\pi}{6}, \frac{\pi}{3}\right]$ and $\left[\frac{\pi}{3}, \frac{\pi}{2}\right]$. Using (17), we have $\forall t \in \left[0, \frac{\pi}{6}\right]$ that $|v_0(t)|$ $= \frac{1}{3}\left|0 + v\left(\frac{\pi}{3} - t\right) - v\left(\frac{\pi}{3} + t\right)\right| \leq \frac{1}{3} \max_{t \in \left[0 \quad \frac{\pi}{6}\right]} \left|v\left(\frac{\pi}{3} - t\right) - v\left(\frac{\pi}{3} + t\right)\right| = \frac{1}{3}\max\{|0 -$ $0|, |1-1|, |1-0|, |0-1|\} = \frac{1}{3}$ □

Proposition 2 *For a 3-level OPP, if* $\alpha_N \leq \frac{\pi}{3}$ *and N is odd, then* $|v_0(t)| \leq \frac{1}{3}$.

Proof. If $\alpha_N \leq \frac{\pi}{3}$ and N is odd, then $v(t) = 1$, $\forall t \in \left[\frac{\pi}{3}, \frac{\pi}{2}\right]$, and the value of $v(t)$ is either 0 or 1 on the intervals $\left[0, \frac{\pi}{6}\right]$ and $\left[\frac{\pi}{6}, \frac{\pi}{3}\right]$. Using (17), we have $\forall t \in \left[0, \frac{\pi}{6}\right]$ that

$$\begin{aligned} |v_0(t)| &= \frac{1}{3}\left|v(t) + v\left(\frac{\pi}{3} - t\right) - 1\right| \\ &\leq \frac{1}{3} \max_{t \in \left[0, \frac{\pi}{6}\right]} \left|v(t) + v\left(\frac{\pi}{3} - t\right) - 1\right| = \frac{1}{3} \end{aligned}$$

□

For an odd value of N, we can strengthen the previous results and combine them into a single case, as discussed next.

Proposition 3 *For a 3-Level OPP with an odd pulse number N, if*

$$\alpha_N - \alpha_1 \leq \frac{\pi}{3}, \tag{18}$$

then $|v_0(t)| \leq \frac{1}{3}$.

Proof. The cases in which $\alpha_1 \geq \frac{\pi}{6}$ or $\alpha_N \leq \frac{\pi}{3}$ have been shown in the previous two propositions. So, it remains to show the case when $\alpha_1 \in \left[0, \frac{\pi}{6}\right]$ and $\alpha_N \in \left[\frac{\pi}{3}, \frac{\pi}{2}\right]$. In this latter case, (18) implies $|v_0(t)| = \max\left(\max_{t \in \left[0, \alpha_N - \frac{\pi}{3}\right]} \{\frac{1}{3}\left|v\left(\frac{\pi}{3} - t\right) - v\left(\frac{\pi}{3} + t\right)\right|,\right.$ $\left.\max_{t \in \left[\alpha_N - \frac{\pi}{3}, r\frac{\pi}{6}\right]} \left\{\frac{1}{3}\left|v(t) + v\left(\frac{\pi}{3} - t\right) - 1\right|\right\}\right) \leq \frac{1}{3}$. An illustration of the proof is shown in Figure 3. □

4 Numerical Results

4.1 3-Level OPPs

In order to illustrate the degree of conservatism introduced by all the foremen-tioned approximations of the CMV constraint, we shall focus on the 3-level OPPs, i.e., $L = 3$, for which we can illustrate all the results in the previous section. The pulse number is taken to be $N = 3$ in order to allow us to visualize the results in 3D, the bound on the CMV constraint is taken to be $\gamma = \frac{1}{3}$, and the minimal separation between the switching angles is taken to be $\delta = 0$. The feasible set consisting of the intersection of CMV constraint set (11) and the constraint set generated by (9) is depicted in 4 below. The obtained set is a truncation of the otherwise tetrahedral set. Note that for this case the number of feasible structures

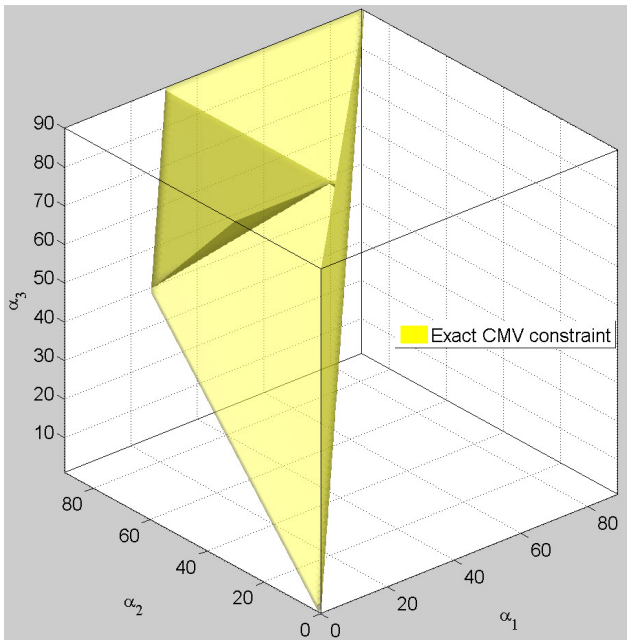

Figure 4: The intersection of the constraints (11) and (9), with $\gamma = \frac{1}{3}$ and $\delta = 0$.

is one, and is given by $\bar{f} = \begin{bmatrix} 1 & -1 & 1 \end{bmatrix}$.

4.1.1 ℓ_1-Norm Approximation

In comparison, the set induced by the ℓ_1-norm constraint (14) with $\gamma = \frac{1}{3}$ is depicted in Figure 5. Obviously, one has a conservative approximation of the set obtained with an exact CMV constraint. However, most of this conservatism can be eliminated by relaxing the ℓ_1-norm constraint (14), i.e., increasing the bound

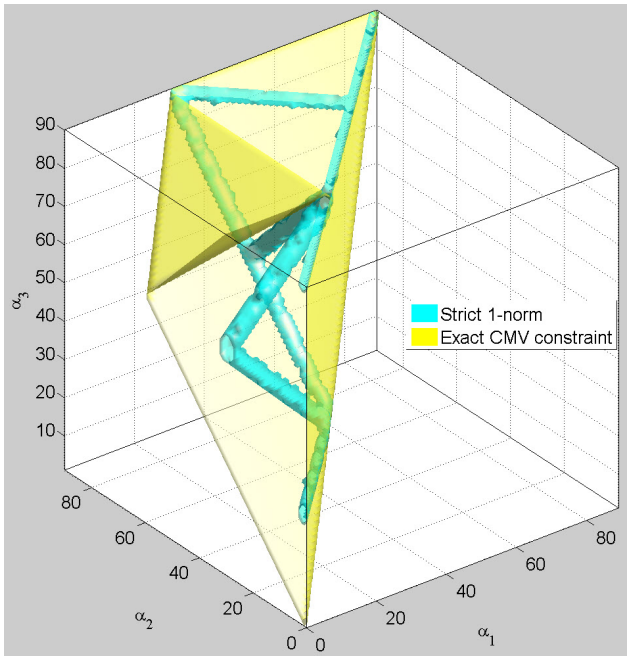

Figure 5: Illustration of the conservatism of the ℓ_1-norm constraint (14) with $\gamma = \frac{1}{3}$ versus the original CMV constraint (11). Both constraints were intersected with (9).

γ and then post-processing the obtained result with the original CMV constraint (11) with $\gamma = \frac{1}{3}$. The obtained set with $\gamma = 1$ in (14) is depicted in Figure 6. It is easily seen that by adopting such a relaxation of the bound γ almost the total original feasible set is recovered.

4.1.2 ℓ_2-Norm Approximation

The set induced by the ℓ_2-norm constraint (16) with $\gamma = \frac{1}{3}$ is depicted in Figure 7. Again, one has a conservative approximation set with respect to the one obtained with an exact CMV constraint, as well as with respect to the one obtained with the ℓ_1 constraint. However, most of this conservatism can be eliminated by relaxing the ℓ_2-norm constraint (16), i.e., increasing the bound γ and then post-processing the obtained result with the original CMV constraint (11) and $\gamma = \frac{1}{3}$. The obtained set with $\gamma = 1$ in (16) is depicted in Figure 8. It is easily seen that by adopting such a relaxation of the bound γ the total original feasible set is almost fully recovered.

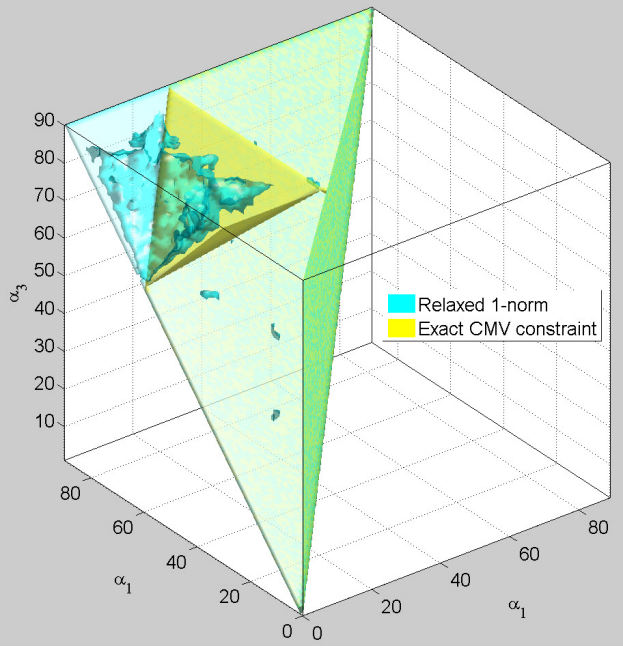

Figure 6: Illustration of the relaxed ℓ_1-norm constraint (14) with $\gamma = 1$ versus the original CMV constraint (11). Both constraints were intersected with (9).

4.1.3 60° constraint

As we have a 3-level OPPs with an odd pulse number $N = 3$, we can apply the constraint (18) instead of the original CMV constraint (11). The result is depicted in Figure 9. It shows that one can actually recover almost the whole set which is given by the intersetction of (11) with the minimal separation constraint (9).

4.2 5-Level OPPs

In this section, we focus of the loss of performance, i.e., TDD_i, when we include the CMV constraint (11). We set the pulse number $N = 8$ and in evaluating the THD_i we use the parameters $l_\sigma = 18.8$ mH and $I_{rat} = 137$ A. The optimization was run for the case where the CMV constraint (11) was not used and for the case where the ℓ_1 constraint approximation (14) was used. In the latter case, we adopted the strategy of relaxing the bound γ and post-processing the obtained result in order to ensure that the original CMV constraint (11) is satisfied. The relative increase in the TDD_i value due to the enforcement of the CMV constraint is shown in Figure 10. Notice that the additional CMV constraint does not substantially increase the obtained TDD_i. It is also important to note that at high modulation indices above $m = 1.179$ the optimization problem with the CMV constraint

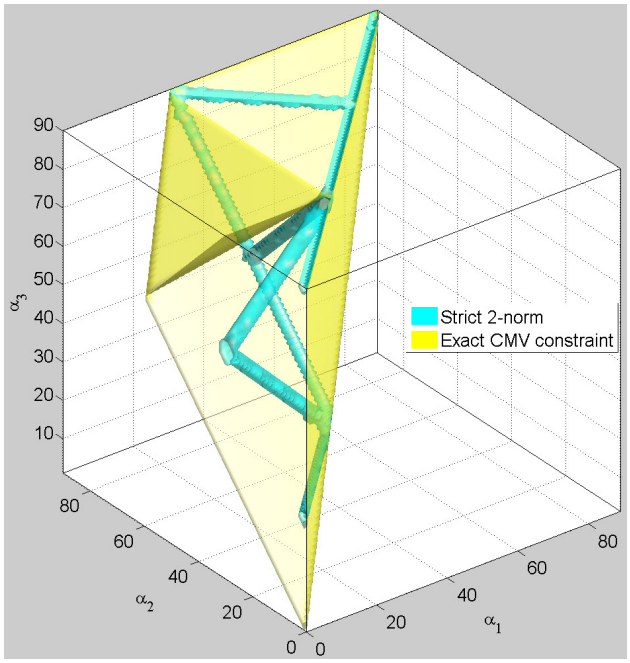

Figure 7: Illustration of the conservatism of the ℓ_2-norm constraint (16) with $\gamma = \frac{1}{3}$ versus the original CMV constraint (11). Both constraints were intersected with (9).

is not feasible anymore, while the one without the CMV constraint remains feasible but the TDD_i drastically deteriorates as the modulation index approaches its maximal value at $\frac{4}{\pi}$. In the case of $N = 8$ the number of different possible structures is 16. Not that this OPP would be applicable within the range $m \in [0.7,\ 1.1]$, and in this range the relative increase in the TDD_i due to the inclusion of the CMV constraint is bounded by approx. 40%.

5 Conclusions and Future Work

We studied the problem of computing Optimized Pulse Patterns (OPPs) for multiple level converters with quarter wave symmetry and constraints on the common mode voltage (CMV). We provided various ways of approximating the CMV constraint based on various norm approximations. We also provided a less conservative result for the 3-level OPPs case. We have shown via numerical illustrations the additional conservatism that is added by the various approximations of the CMV constraint, as well as the performance loss due to this CMV constraint. Future work will be targeted towards obtaining results for the L-level OPPs similar to the less conservative results that we obtained for the 3-level case in this article.

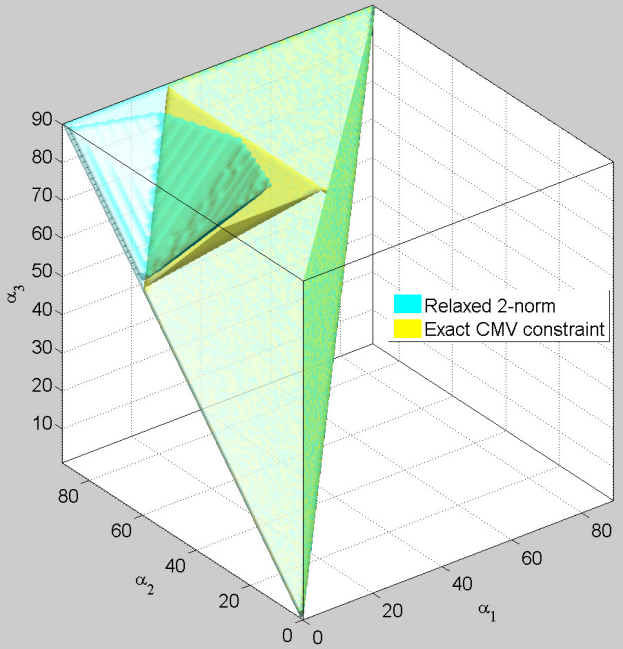

Figure 8: Illustration of the relaxed ℓ_2-norm constraint (16) with $\gamma = 1$ versus the original CMV constraint (11). Both constraints were intersected with (9).

References

Agelidis, V.G., Balouktsis, A.I., and Dahidah, M.S.A. (2008). A five-level symmetrically defined selective harmonic elimination PWM strategy: Analysis and experimental validation. *IEEE Trans. Pow. Elect.*, 23(1), 19–26.

Buja, G.S. (1980). Optimum output waveforms in PWM inverters. *IEEE Trans. Ind. Appl.*, 16(6), 830–836.

Chiasson, J.N., Tolbert, L.M., McKenzie, K.J., and Du, Z. (2008). A complete solution to the harmonic elimination problem. *IEEE Trans. Pow. Elect.*, 19(2), 491–499.

Fei, W., Ruan, X., and Wu, B. (2009). A generalized formulation of quarter-wave symmetry she-pwm problems for multilevel inverters. *IEEE Trans. Power Elect.*, 7(24), 1758–1766.

Geyer, T., Kieferndorf, F., Papafotiou, G., and Oikonomou, N. (2010). Method for controlling a converter. EP 2 469 692 A1.

Geyer, T., Oikonomou, N., Papafotiou, G., and Kieferndorf, F. (2012). Model predictive pulse pattern control. 48(2), 663–676.

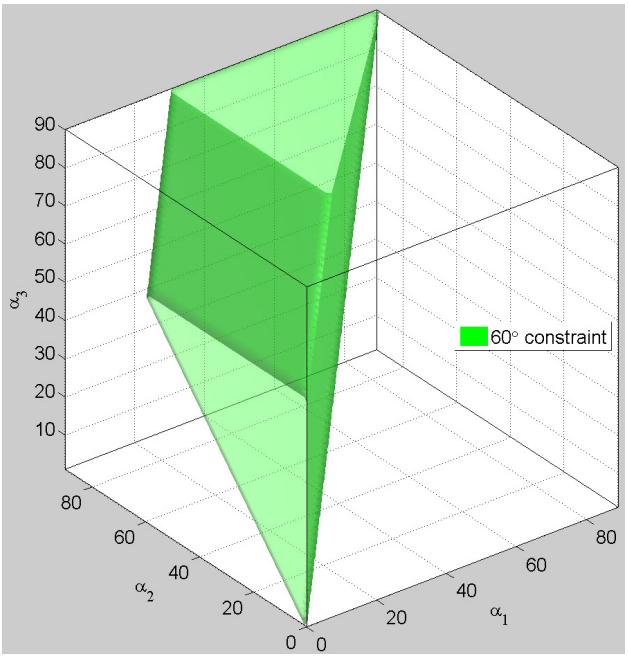

Figure 9: Illustration of the conservative feasible set obtained with the constraint (18) versus the original CMV constraint for $N = 3$ and $L = 3$.

Holmes, D.G. and Lipo, T.A. (2003). *Pulse Width Modulation for Power Converters: Principles and Practice*. Wiley-IEEE Press.

Holtz, J. and Beyer, B. (1991). Off-line optimized synchronous pulsewidth modulation with on-line control during transients. 1(3), 193–200.

Holtz, J. and Beyer, B. (1995). Fast current trajectory tracking control based on synchronous optimal pulsewidth modulation. 31(5), 1110–1120.

Holtz, J. and Oikonomou, N. (2007). Synchronous optimal pulsewidth modulation and stator flux trajectory control for medium-voltage drives. 43(2), 600–608.

Holtz, J. and Qi, X. (2013). Optimal control of medium-voltage drives – an overview. *IEEE Trans. Ind. Elect.*, 60(12), 5472–5481.

Khalil, H.K. (2001). *Nonlinear Systems*. Prentice Hall. 3rd Ed.

Meili, J., Ponnaluri, S., Serpa, L., Steimer, P., and Kolar, J. (2006). Optimized pulse patterns for the 5-level ANPC converter for high speed high power applications. 2587–2592.

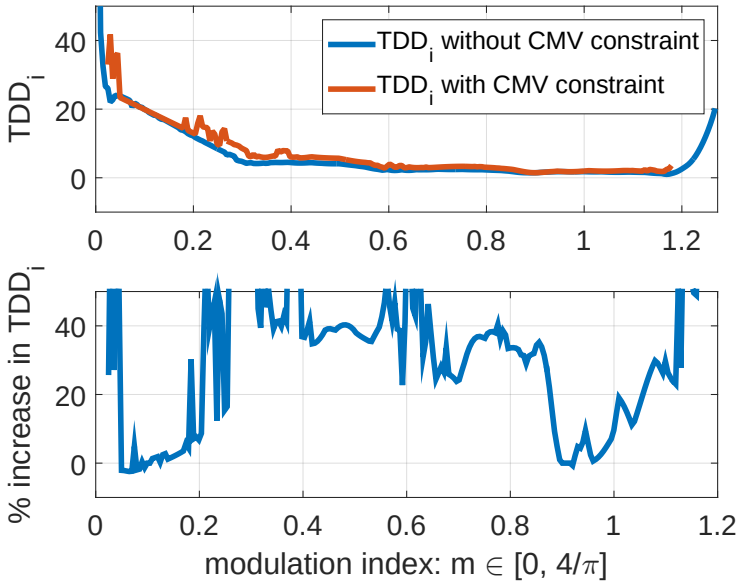

Figure 10: Normalized TDD_i values (11) (top) and relative increase in the value of the current TDD_i (bottom), due to inclusion of the CMV constraint for $N = 8$.

Rathore, A.K., Holtz, J., and Boller, T. (2013). Generalized optimal pulsewidth modulation of multilevel inverters for low-switching-frequency control of medium-voltage high-power industrial ac drives. *IEEE Trans. Ind. Elect.*, 60(12), 5472–5481.

A

A.1 Derivation of (4)

The general expression for the Fourier series odd coefficients (due to the quarter wave symmetry we have only odd coefficients) is given by

$$\begin{aligned}
\hat{v}_k &= \frac{2}{2\pi}\int_0^{2\pi} v(\tau)\sin(k\tau)d\tau \\
&= \frac{4}{\pi}\int_0^{\frac{\pi}{2}} v(\tau)\sin(k\tau)d\tau \\
&= \frac{4}{\pi}\frac{u_d}{L-1}\left\{\int_{\alpha_1}^{\alpha_2} f_1\sin(k\tau)d\tau + \int_{\alpha_2}^{\alpha_3}(f_1+f_2)\sin(k\tau)d\tau\right. \\
&\quad \left. +\cdots+\int_{\alpha_N}^{\frac{\pi}{2}}(f_1+f_2+\cdots f_N)\sin(k\tau)d\tau\right\} \\
&= \frac{4}{\pi}\frac{u_d}{L-1}\frac{1}{k}\Big\{f_1(\cos(k\alpha_1)-\cos(k\alpha_2))+ \\
&\qquad\qquad (f_1+f_2)(\cos(k\alpha_2)-\cos(k\alpha_3))+ \\
&\qquad\qquad (f_1+f_2+\cdots+f_N)(\cos(k\alpha_N)-\cos(k\frac{\pi}{2}))\Big\}, \qquad (19)
\end{aligned}$$

where the second equality follows from the fact that $v(t)$ is quarter wave symmetric and k is odd. Finally, simplifying the last expression (19) yields the expression (4).

A.2 Proof of (10)

Assume that the three phase symmetry condition (2) holds, and consider the Fourier series expansion in (3). Then, the CMV is given by

$$\begin{aligned}
v_0(t) &= \frac{1}{3}\left(v_a(t)+v_b(t)+v_c(t)\right) \\
&= \frac{1}{3}\sum_{k=1,3,5,\cdots}\hat{v}_k\left(\sin(kt)+\sin(k(t-\frac{2\pi}{3}))+\sin(k(t+\frac{2\pi}{3}))\right) \\
&= \frac{1}{3}\sum_{k=1,3,5,\cdots}\hat{v}_k\left(\sin(kt)+2\cos(k\frac{2\pi}{3})\sin(kt)\right) \\
&= \sum_{k=3,9,15,\ldots\cdots}\hat{v}_k\sin(kt),
\end{aligned}$$

where we have used the fact that

$$\cos(k\frac{2\pi}{3}) = \begin{cases} 1, & \forall k = 3,9,15,\cdots \\ -\frac{1}{2}, & \forall k = 1,5,7,\cdots \end{cases}$$

Defining $\mathbb{H}_0 = \{3, 9, 15, 21, 27, \cdots\}$ completes the derivation.

A.3 v_0 is quarter wave symmetric with period $\frac{2\pi}{3}$

The fact that v_0 has a period $\frac{2\pi}{3}$ is obvious from (10). To show that the CMV is quarter wave symmetric, we need to show the following two conditions

$$\begin{cases} v_0(t) = v_0(\frac{\pi}{3} - t), & \forall t \in \left[0, \quad \frac{\pi}{6}\right], \\ v_0(t) = -v_0(\frac{2\pi}{3} - t), & \forall t \in \left[0, \quad \frac{\pi}{3}\right]. \end{cases}$$

First, we show that

$$\begin{aligned} v_0(t) - v_0(\frac{\pi}{3} - t) &= \sum_{k \in \mathbb{H}_0} \hat{v}_k \left(\sin(kt) - \sin(k(\frac{\pi}{3} - t)) \right) \\ &= \sum_{k \in \mathbb{H}_0} \hat{v}_k \left(\sin(kt) - \sin(k\frac{\pi}{3})\cos(kt) + \cos(k\frac{\pi}{3})\sin(kt) \right) \\ &= 0, \end{aligned} \tag{20}$$

since $\sin(k\frac{\pi}{3}) = 0$ and $\cos(k\frac{\pi}{3}) = -1$ for $k \in \mathbb{H}_0$.

Second, we have that

$$\begin{aligned} v_0(t) + v_0(\frac{2\pi}{3} - t) &= \sum_{k \in \mathbb{H}_0} \hat{v}_k \left(\sin(kt) + \sin(k(\frac{2\pi}{3} - t)) \right) \\ &= \sum_{k \in \mathbb{H}_0} \hat{v}_k \left(\sin(kt) + \sin(k\frac{2\pi}{3})\cos(kt) - \cos(k\frac{2\pi}{3})\sin(kt) \right) \\ &= 0, \end{aligned} \tag{21}$$

since $\sin(k\frac{2\pi}{3}) = 0$ and $\cos(k\frac{2\pi}{3}) = 1$ for $k \in \mathbb{H}_0$.

A.4 Derivation of (17)

$$\begin{aligned} &\frac{1}{3}\left(v(t) + v\left(\frac{\pi}{3} - t\right) - v\left(\frac{\pi}{3} + t\right) \right) \\ &= \frac{1}{3} \sum_{k=1,3,5,\cdots} \hat{v}_k \left(\sin(kt) + \sin(k(\frac{\pi}{3} - t)) - \sin(k(\frac{\pi}{3} + t)) \right) \\ &= \frac{1}{3} \sum_{k=1,3,5,\cdots} \hat{v}_k \left(\sin(kt) - 2\cos(k\frac{\pi}{3})\sin(kt) \right) \\ &= \sum_{k=3,9,15,\ldots\cdots} \hat{v}_k \sin(kt), \end{aligned}$$

where we have used the fact that

$$\cos(k\frac{\pi}{3}) = \begin{cases} -1, & \forall k = 3,9,15,\cdots \\ \frac{1}{2}, & \forall k = 1,5,7,11,\cdots \end{cases}$$